

## Leading-order hadronic contribution to the electron and muon $g - 2$

Fred Jegerlehner<sup>1,2,a</sup>

<sup>1</sup>Deutsches Elektronen-Synchrotron (DESY), Platanenallee 6, D-15738 Zeuthen, Germany

<sup>2</sup>Humboldt-Universität zu Berlin, Institut für Physik, Newtonstrasse 15, D-12489 Berlin, Germany

**Abstract.** I present a new data driven update of the hadronic vacuum polarization effects for the muon and the electron  $g - 2$ . For the leading order contributions I find  $a_\mu^{\text{had}(1)} = (688.57 \pm 4.28)[688.91 \pm 3.52] \times 10^{-10}$  based on  $e^+e^-$  data [incl.  $\tau$  data],  $a_\mu^{\text{had}(2)} = (-9.92 \pm 0.10) \times 10^{-10}$  (NLO) and  $a_\mu^{\text{had}(3)} = (1.23 \pm 0.01) \times 10^{-10}$  (NNLO) for the muon, and  $a_e^{\text{had}(1)} = (185.11 \pm 1.24) \times 10^{-14}$  (LO),  $a_e^{\text{had}(2)} = (-22.15 \pm 0.16) \times 10^{-14}$  (NLO) and  $a_e^{\text{had}(3)} = (2.80 \pm 0.02) \times 10^{-14}$  (NNLO) for the electron. A problem with vacuum polarization undressing of cross-sections (time-like region) is addressed. I also add a comment on properly including axial mesons in the hadronic light-by-light scattering contribution. My estimate here reads  $a_\mu[a_1, f'_1, f_1] \sim (7.51 \pm 2.71) \times 10^{-11}$ . With these updates  $a_\mu^{\text{exp}} - a_\mu^{\text{the}} = (31.0 \pm 8.2) \times 10^{-10}$  a  $3.8 \sigma$  deviation, while  $a_e^{\text{exp}} - a_e^{\text{the}} = (-1.14 \pm 0.82) \times 10^{-12}$  shows no significant deviation.

### 1 Introduction: hadronic effects in $g - 2$ .

A well known general problem in electroweak precision physics are the higher order contributions from hadrons (quark loops) at low energy scales. While leptons primarily exhibit the fairly weak electromagnetic interaction, which can be treated in perturbation theory, the quarks are strongly interacting via confined gluons where any perturbative treatment breaks down. Considering the lepton anomalous magnetic moments one distinguishes three types of non-perturbative corrections: **(a)** Hadronic Vacuum Polarization (HVP) of order  $O(\alpha^2)$ ,  $O(\alpha^3)$ ,  $O(\alpha^4)$ ; **(b)** Hadronic Light-by-Light (HLbL) scattering at  $O(\alpha^3)$ ; **(c)** hadronic effects at  $O(\alpha G_F m_\mu^2)$  in 2-loop electroweak (EW) corrections, in all cases quark-loops appear as hadronic “blobs”. The hadronic contributions are limiting the precision of the predictions.

Evaluation of non-perturbative effects is possible by using experimental data in conjunction with Dispersion Relations (DR), by low energy effective modeling via a Resonance Lagrangian Approach (RLA) (Vector Meson Dominance (VMD) implemented in accord with chiral structure of QCD) [1–3], like the Hidden Local Symmetry (HLS) or the Extended Nambu Jona-Lasinio (ENJL) models, or by lattice QCD. Specifically: **(a)** HVP via a dispersion integral over  $e^+e^- \rightarrow \text{hadrons}$  data (1 independent amplitude to be determined by one specific data channel) (see e.g. [4]) as elaborated below, by the HLS effective Lagrangian approach [5–9], or by lattice QCD [10–15]; **(b)** HLbL via a RLA together with operator product expansion (OPE) methods [16–19], by a dispersive approach using  $\gamma\gamma \rightarrow \text{hadrons}$  data (28 independent amplitudes to be determined by as many independent data sets in prin-

ciple) [20–22] or by lattice QCD [23, 24]; **(c)** EW quark-triangle diagrams are well under control, because the possible large corrections are related to the Adler-Bell-Jackiw (ABJ) anomaly which is perturbative and non-perturbative at the same time. Since  $VVV = 0$  by the Furry theorem, only VVA (of  $\gamma\gamma Z$ -vertex, V=vector, A=axialvector) contributes. In fact leading effects are of short distance type ( $M_Z$  mass scale) and cancel against lepton-triangle loops (anomaly cancellation) [25, 26].

### 2 Leading-order $a_\mu^{\text{had}}$ via $\sigma(e^+e^- \rightarrow \text{hadrons})$

The leading *non-perturbative* hadronic contribution to  $a_\mu^{\text{had}}$ , represented by the diagram figure 1, can be obtained

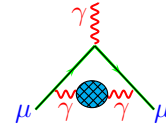


**Figure 1.** Leading diagram exhibiting a hadronic “blob”.

in terms of undressed experimental cross-sections data

$$R_\gamma(s) \equiv \sigma^{(0)}(e^+e^- \rightarrow \gamma^* \rightarrow \text{hadrons}) / \frac{4\pi\alpha^2}{3s}, \quad (1)$$

$s = E_{\text{cm}}^2$ ,  $E_{\text{cm}}$  the center of mass energy, and the DR:

$$a_\mu^{\text{had}} = \left(\frac{\alpha m_\mu}{3\pi}\right)^2 \left( \int_{4m_\pi^2}^{E_{\text{cut}}^2} ds \frac{R_\gamma^{\text{data}}(s) \hat{K}(s)}{s^2} + \int_{E_{\text{cut}}^2}^{\infty} ds \frac{R_\gamma^{\text{pQCD}}(s) \hat{K}(s)}{s^2} \right). \quad (2)$$

<sup>a</sup>e-mail: fjeger@physik.hu-berlin.de

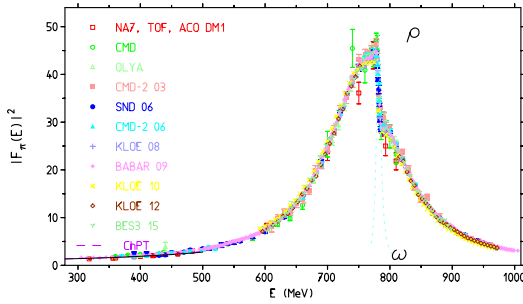


**Figure 2.** The pion form factor  $|F_\pi(s)|^2 = 4R_{\pi\pi}/\beta_\pi^3$  ( $\beta_\pi = \sqrt{1 - 4m_\pi^2/s}$ ) dominated by the  $\rho$  resonance peak. Data include measurements from Novosibirsk (NSK) [27–29], Frascati (KLOE) [30–32], SLAC (BaBar) [33] and Beijing (BESIII) [34].

**Table 1.** Results for  $a_\mu^{\text{had}(1)}$  (in units  $\times 10^{-10}$ ).

final state	range (GeV)	$a_\mu^{\text{had}(1)}$ (stat) (syst) [tot]	rel abs %
$\rho$	(0.28, 1.05)	507.55 (0.39) (2.68) [2.71]	0.5 [39.9]
$\omega$	(0.42, 0.81)	35.23 (0.42) (0.95) [1.04]	3.0 [ 5.9]
$\phi$	(1.00, 1.04)	34.31 (0.48) (0.79) [0.92]	2.7 [ 4.7]
$J/\psi$		8.94 (0.42) (0.41) [0.59]	6.6 [ 1.9]
$\Upsilon$		0.11 (0.00) (0.01) [0.01]	6.8 [ 0.0]
had	(1.05, 2.00)	60.45 (0.21) (2.80) [2.80]	4.6 [42.9]
had	(2.00, 3.10)	21.63 (0.12) (0.92) [0.93]	4.3 [ 4.7]
had	(3.10, 3.60)	3.77 (0.03) (0.10) [0.10]	2.8 [ 0.1]
had	(3.60, 5.20)	7.50 (0.04) (0.01) [0.04]	0.3 [ 0.0]
pQCD	(5.20, 9.46)	6.27 (0.00) (0.01) [0.01]	0.0 [ 0.0]
had	(9.46, 13.00)	1.28 (0.01) (0.07) [0.07]	5.4 [ 0.0]
pQCD	(13.0, $\infty$ )	1.53 (0.00) (0.00) [0.00]	0.0 [ 0.0]
data	(0.28, 13.00)	680.77 (0.89) (4.19) [4.28]	0.6 [100.]
total		688.57 (0.89) (4.19) [4.28]	0.6 [100.]

The kernel  $\hat{K}(s)$  is an analytically known monotonically increasing function, raising from about 0.64 at the two pion threshold  $4m_\pi^2$  to 1 as  $s \rightarrow \infty$ . This integral is well defined due to the asymptotic freedom of QCD, which allows for a perturbative QCD (pQCD) evaluation of the high energy contributions. Because of the  $1/s^2$  weight, the dominant contribution comes from the lowest lying hadronic resonance, the  $\rho$  meson (see figure 2). As low energy contributions are enhanced, about  $\sim 75\%$  come from the region  $2m_\pi < \sqrt{s} < 1$  GeV dominated by the  $\pi^+\pi^-$  channel. Experimental errors imply theoretical uncertainties, the main issue for the muon  $g-2$ . Typically, results are collected from different resonances and regions as presented in table 2. Statistical errors (stat) are summed in quadrature, systematic (syst) ones are taken into account linearly (100% correlated) within the different contributions of the list, and summed quadratically from the different regions and resonances. From 5.2 GeV to 9.46 GeV and above 13 GeV pQCD is used. Relative (rel) and absolute (abs) errors are also shown. The distribution of contributions and errors are illustrated in the pie chart figure 3. As a result we find

$$a_\mu^{\text{had}(1)} = (688.57 \pm 4.28)[688.91 \pm 3.52] \times 10^{-10} \quad (3)$$

based on  $e^+e^-$ -data [incl.  $\tau$ -decay spectra [35]]. In the last 15 years  $e^+e^-$  cross-section measurements have dramatically improved, from energy scans [27–29] at Novosibirsk (NSK) and later, using the radiative return mecha-

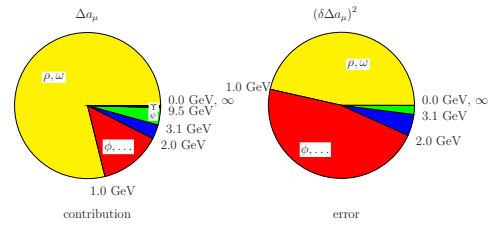


**Figure 3.** Muon  $g-2$ : distribution of contributions and error squares from different energy ranges.

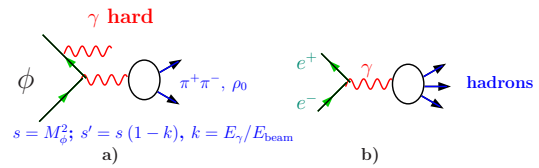


**Figure 4.** a) Initial state radiation (ISR), b) Standard energy scan.

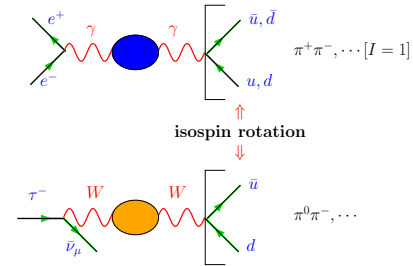


**Figure 5.**  $\tau$ -decay data may be combined with  $I=1$  part of  $e^+e^-$  annihilation data after isospin rotation  $[\pi^-\pi^0] \leftrightarrow [\pi^-\pi^+]$  and applying isospin breaking (IB) corrections (e.m. effects, phase space, isospin breaking in masses, widths,  $\rho^0 - \omega$  mixing etc.).

nism, measurements via initial state radiation (ISR) at meson factories (see figure 4) [30–34]. A third possibility to enhance experimental information useful to improve HVP estimates are  $\tau$ -decay spectra  $\tau \rightarrow \bar{\nu}_\tau \pi^0 \pi^-, \dots$ , supplied by isospin breaking effects [5–7, 35–40]. In the conserved vector current (CVC) limit  $\tau$  spectra should be identical to the isovector part  $I = 1$  of the  $e^+e^-$  spectra, as illustrated in figure 5. Including the  $I = 1$   $\tau \rightarrow \pi\pi\nu_\tau$  data available from [41–45] in the range [0.63–0.96] GeV one obtains [35]:

$$\begin{aligned} a_\mu^{\text{had}}[ee \rightarrow \pi\pi] &= 353.82(0.88)(2.17)[2.34] \times 10^{-10} \\ a_\mu^{\text{had}}[\tau \rightarrow \pi\pi\nu] &= 354.25(1.24)(0.61)[1.38] \times 10^{-10} \\ a_\mu^{\text{had}}[ee + \tau] &= 354.14(0.82)(0.86)[1.19] \times 10^{-10}, \end{aligned}$$

which improves the LO HVP as given in (3). We briefly summarize recent progress in data collection as follows.

## 2.1 Data

As I mentioned the most important data are the  $\pi\pi$  production data in the range up to 1 GeV. New experimental

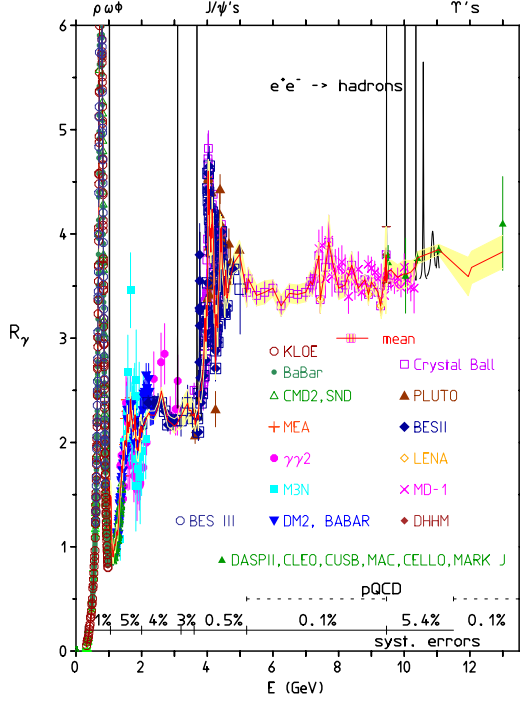


**Figure 6.** My 2015 compilation of  $R_\gamma$  as a function of energy  $E$ .

input for HVP comes from BESIII [34]. Still the most precise ISR measurements from KLOE and BaBar are in conflict, but the new ISR data from BESIII steps to resolve this tension, as it lies in between the two. Other data recently collected, and published up to the end of 2014, include the  $e^+e^- \rightarrow 3(\pi^+\pi^-)$  data from CMD-3 [46], the  $e^+e^- \rightarrow \omega\pi^0 \rightarrow \pi^0\pi^0\gamma$  from SND [47] and several data sets collected by BaBar in the ISR mode<sup>1</sup> [48–51]. These data samples highly increase the available statistics for the annihilation channels opened above 1 GeV and lead to significant improvements. Recent/preliminary results also included are  $e^+e^- \rightarrow \pi^+\pi^-\pi^0$  from Belle,  $e^+e^- \rightarrow K^+K^-$  from CMD-3,  $e^+e^- \rightarrow K^+K^-$  from SND. The resulting data sample is collected in figure 6, which has indicated the overall precision of the different ranges as well as the pQCD ranges, where data are replaced by pQCD results. Still one of the main issue in HVP is  $R_\gamma(s)$  in the region 1.2 to 2.4 GeV, which actually has been improved dramatically by the exclusive channel measurements by BaBar in the last decade. The most important 20 out of more than 30 channels are measured, many known at the 10 to 15% level. The exclusive channel therefore has a much better quality than the very old inclusive data from Frascati (see figure 7).

## 2.2 NLO and NNLO HVP effects updated

The next-to-leading order (NLO) HVP is represented by diagrams in figure 8. With kernels from [53], the results of an updated evaluation are presented in table 2. The next-to-next leading order (NNLO) contributions have

<sup>1</sup>Including the  $p\bar{p}$ ,  $K^+K^-$ ,  $K_L K_S$ ,  $K_L K_S \pi^+\pi^-$ ,  $K_S K_S \pi^+\pi^-$ ,  $K_S K_S K^+K^-$  final states.

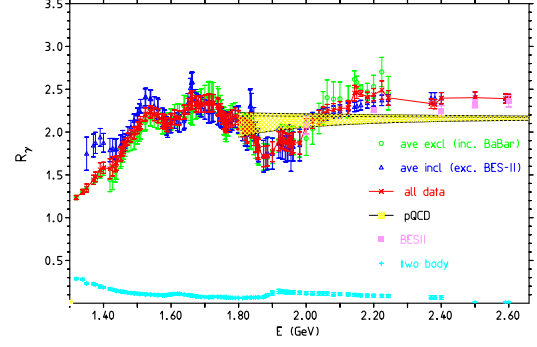


**Figure 7.**  $e^+e^-$  annihilation data in the 1.4 to 2.6 GeV region. Summed up exclusive (excl) channel data are shown together with old inclusive data (incl). Two-body channels represent a small fraction of  $R_\gamma$  only. Above 2 GeV good quality inclusive BES-II data [52] provide a fairly well determined  $R_\gamma(s)$ .

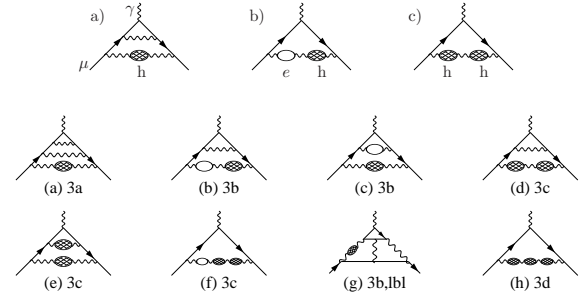


**Figure 8.** Feynman diagrams with hadronic insertions at NLO (top row) and NNLO.

**Table 2.** NLO contributions diagrams a) - c) (in units  $10^{-11}$ )

$a_\mu^{(2a)}$	$a_\mu^{(2b)}$	$a_\mu^{(2c)}$	$a_\mu^{\text{had}(2)}$
-206.10(1.73)	103.55(0.73)	3.38(0.05)	-99.17 (1.00)

**Table 3.** NNLO contributions diagrams (a) - (h) (in units  $10^{-11}$ )

Class	Kurz et al [54]	my evaluation
$a_\mu^{(3a)}$	=	8.0 7.82(77)
$a_\mu^{(3b)}$	=	-4.1 -4.03(37)
$a_\mu^{(3b,1bl)}$	=	9.1 9.00(77)
$a_\mu^{(3c)}$	=	-0.6 -0.544(7)
$a_\mu^{(3d)}$	=	0.005 0.00522(15)
$a_\mu^{\text{had}(3)}$	=	12.4(1) 12.25(12)

been calculated recently [54, 55]. Diagrams are shown in figure 8 and corresponding contributions evaluated with kernels from [54] are listed in table 3.

The challenge for the future is to keep up with the future experiments [56], which will improve the experimental accuracy from  $\delta a_\mu^{\text{exp}} = 63 \times 10^{-11} [\pm 0.54 \text{ ppm}]$  at present to  $\delta a_\mu^{\text{exp}} = 16 \times 10^{-11} [\pm 0.14 \text{ ppm}]$  the next years. The present results  $a_\mu^{\text{had}}[\text{LO VP}] = (6889 \pm 35) \times 10^{-11}$  amount to  $+59.09 \pm 0.30 \text{ ppm}$ , which poses the major challenge. The subleading results  $a_\mu^{\text{had}}[\text{NLO VP}] = (-99.2 \pm$

$1.0) \times 10^{-11}$  and  $a_\mu^{\text{had}}[\text{NNLO VP}] = (12.4 \pm 0.1) \times 10^{-11}$  although relevant will be known well enough. These number also compare with the well established weak  $a_\mu^{\text{EW}} = (154 \pm 1) \times 10^{-11}$  and the problematic HLbL estimated to contribute  $a_\mu^{\text{had,HLbL}} = [(105 \div 106) \pm (26 \div 39)] \times 10^{-11}$ , which is representing a  $+0.90 \pm 0.28$  ppm effect. Next generation experiments require a factor 4 reduction of the uncertainty optimistically feasible should be a factor 2 we hope.

### 3 Effective field theory: the Resonance Lagrangian Approach

As we know HVP is dominated by spin 1 resonance physics, therefore we need a low energy effective theory which includes  $\rho, \omega, \phi$  mesons. Principles to be implemented are the VMD mechanism, the chiral structure of QCD (chiral perturbation theory), and electromagnetic gauge invariance. A specific realization is the HLS effective Lagrangian [57] (see [8] for a brief account). In our context it has been first applied to HLbL of muon  $g - 2$  in [1], to HVP in [58]. Largely equivalent is the ENJL model on which the most complete analysis of HLbL in [2] was based. To actually work in practice, the HLS symmetry has to be broken by phenomenologically well known  $SU(3)$  and  $SU(2)$  flavor breaking and the framework we consider here is the broken HLS (BHLS) model.

We briefly outline the BHLS global fit strategy of a HVP evaluation [9]: one uses data below  $E_0 = 1.05$  GeV (just including the  $\phi$ ) to constrain the effective Lagrangian couplings, using 45 different data sets (6 annihilation channels and 10 partial width decays). The effective theory then can be used to predict cross-sections mainly for two-body reactions (besides  $3\pi$ )

$$\pi^+\pi^-, \pi^0\gamma, \eta\gamma, \eta'\gamma, \pi^0\pi^+\pi^-, K^+K^-, K^0\bar{K}^0,$$

while the missing part  $4\pi, 5\pi, 6\pi, \eta\pi\pi, \omega\pi$  as well as the regime  $E > E_0$  is evaluated using data directly and pQCD for perturbative region and tail. Including self-energy effects is mandatory to properly describe  $\rho - \omega - \phi$  mixing and their decays with proper phase space, energy dependent width etc.  $\gamma - V$  ( $V = \rho, \omega, \phi$ ) mixing also turns out to be crucial. The method works in reducing uncertainties by using indirect constraints. It is able to reveal inconsistencies in data, e.g. KLOE vs. BaBar. A goal is to single out a representative effective resonance Lagrangian by a global fit, which is expected to help in improving effective field theory (EFT) calculations of hadronic light-by-light scattering. It has been shown [5–7] that EFT not only helps reducing the uncertainty of HVP, it resolves the  $\tau$  vs.  $e^+e^-$  data puzzle, and it allows us to use, besides the  $e^+e^-$  annihilation data, also the  $\tau$  decay data, as well as other experimental information consistently in a quantum field theory framework. A best fit is obtained for the data configuration NSK+KLOE10+KLOE12+BESIII+ $\tau$  with a result

$$a_\mu^{\text{had}(1)} = (682.40 \pm 3.20) \times 10^{-10}, \quad (4)$$

where  $(569.04 \pm 1.08) \times 10^{-10}$  results from BHLS predicted channels and  $(113.36 \pm 3.01) \times 10^{-10}$  from non-HLS

[thereof  $(112.02 \pm 3.01) \times 10^{-10}$  from data above 1.05 GeV and  $(1.34 \pm 0.11) \times 10^{-10}$  from HLS missing channels below 1.05 GeV]. The global fit including the BABAR sample as well yields  $(685.82 \pm 3.14) \times 10^{-10}$ . In figure 12 we display the global fit BDDJ15\*, the best fit BDDJ15# and BDDJ12 for NSK+ $\tau$ , which includes scan data only.

An important outcome of effective theory modeling of low energy hadron physics is the observation that a unified treatment of different processes on a Lagrangian level is able to resolve [9, 35] the long standing  $\tau$  vs.  $e^+e^- \pi\pi$  data puzzle [37]. The main effect which distort  $e^+e^-$ -spectra relative to  $\tau$ -spectra is  $\rho^0 - \gamma$  interference in the neutral channel, which is absent in charged channel. A minimal model, which allow us to understand this, is VMD II plus scalar QED [35] for the pion-photon interaction, with effective Lagrangian

$$\mathcal{L} = \mathcal{L}_{\gamma\rho} + \mathcal{L}_\pi \quad (5)$$

where

$$\begin{aligned} \mathcal{L}_{\gamma\rho} &= -\frac{1}{4} F_{\mu\nu} F^{\mu\nu} - \frac{1}{4} \rho_{\mu\nu} \rho^{\mu\nu} + \frac{M_\rho^2}{2} \rho_\mu \rho^\mu + \frac{e}{2g_\rho} \rho_{\mu\nu} F^{\mu\nu}, \\ \mathcal{L}_\pi &= D_\mu \pi^+ D^{+\mu} \pi^- - m_\pi^2 \pi^+ \pi^-; \quad D_\mu = \partial_\mu - ieA_\mu - ig_{\rho\pi\pi} \rho_\mu. \end{aligned}$$

Photon and  $\rho$  self-energies are then pion-loops, which also implies non-trivial  $\gamma - \rho^0$  vacuum polarization (see figure 9). The clue is that the  $\rho^0 - \gamma$  mixing is uniquely

**Figure 9.** Irreducible self-energy contribution at one-loop.

fixed by the electronic  $\rho$ -width  $\Gamma_{\rho ee}$ . Nothing unknown to be adjusted! Previous calculations à la Gounaris-Sakurai, considered the mixing term to be constant, i.e.

$-i\Pi_{\gamma\rho}^{\mu\nu}(\pi)(q) = [diagram with a photon loop and a rho loop] + [diagram with a rho loop] \rightarrow [diagram with a photon loop]$ . The problem in comparing charged with neutral channel data turned out to be an inconsistent treatment of quantum loops in the neutral channel Gounaris-Sakurai formula. A consistent calculation requires to consider the  $2 \times 2$  matrix  $\gamma - \rho$  propagator  $D_{\alpha\beta}(s)$  ( $\alpha \in \gamma, \rho, \beta \in \gamma, \rho$ ) as a starting point. The off diagonal  $D_{\gamma\rho}$  element usually has been treated as the well-known VMD  $\gamma - \rho$ -mixing coupling constant. However, one-loop self-energy effects should be included consistently, especially if it turns out that interference effects are large, in spite of the fact that one of the  $g_{\rho\pi\pi}$  couplings in  $D_{\rho\rho}$  is replaced by the electromagnetic charge  $e$  in  $D_{\rho\gamma}$ . In our extended VMD model, properly renormalized, the pion form-factor exhibits the four terms shown in figure 10 such that

$$F_\pi(s) \propto e^2 D_{\gamma\gamma} + eg_{\rho\pi\pi} D_{\gamma\rho} - g_{\rho ee} e D_{\rho\gamma} - g_{\rho ee} g_{\rho\pi\pi} D_{\rho\rho},$$

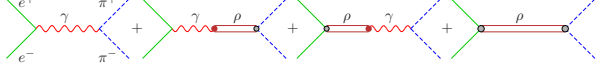


**Figure 10.** Diagrams contributing to the process  $e^+e^- \rightarrow \pi^+\pi^-$ . Propagators are supposed to be corrected for self-energy effects as displayed in figure 9.

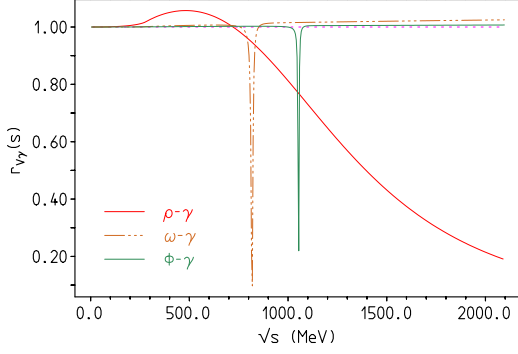


**Figure 11.** The  $\rho^0 - \gamma$  mixing correction to be applied to the  $\tau$  spectral functions. Corresponding effects for  $\omega, \phi$  in  $\pi\pi$  off-resonance are tiny (scaled up  $\Gamma_V/\Gamma(V \rightarrow \pi\pi)$ ). Caution: the model only applies for energies below about  $M_\phi$ . At the  $f_2(1270)$  in  $\gamma\gamma \rightarrow \pi^+\pi^-, \pi^0\pi^0$  one observes the photons to couple to the quarks rather than to point-like pions.

which replaces the  $\rho$  contribution of the GS formula, which usually includes the  $\omega - \rho$  mixing and higher  $\rho$  contributions  $\rho' = \rho(1450)$  and  $\rho'' = \rho(1700)$ . Properly normalized (VP subtraction:  $e^2(s) \rightarrow e^2$ ) we have

$$F_\pi(s) = \left[ e^2 D_{\gamma\gamma} + e(g_{\rho\pi\pi} - g_{\rho ee}) D_{\gamma\rho} - g_{\rho ee} g_{\rho\pi\pi} D_{\rho\rho} \right] / \left[ e^2 D_{\gamma\gamma} \right] \quad (6)$$

Typical couplings are  $g_{\rho\pi\pi}^{\text{bare}} = 5.8935$ ,  $g_{\rho\pi\pi}^{\text{ren}} = 6.1559$ ,  $g_{\rho ee} = 0.018149$ ,  $x = g_{\rho\pi\pi}/g_\rho = 1.15128$  [35].

As a result a correction displayed in figure 11 is obtained, a +5 to -10% correction! The proper relationship between  $e^+e^-$  and  $\tau$  spectral functions

$$v_i(s) = \frac{\beta_i^3(s)}{12\pi} |F_\pi^i(s)|^2 \quad (i = 0, -), \quad (7)$$

in terms of the pion form-factors  $F_\pi$  and the pion velocities  $\beta_i$ , now reads

$$v_0(s) = r_{\rho\gamma}(s) R_{\text{IB}}(s) v_-(s), \quad (8)$$

where  $R_{\text{IB}}(s)$  is the standard isospin breaking correction (see [35, 38–40]). The  $\tau$  requires to be corrected for missing  $\rho - \gamma$  mixing as well, before being used as I=1  $e^+e^-$  data, because results obtained from  $e^+e^-$  data is what goes into the DR (2) (the photon coupled to  $\pi^+\pi^-$  not to  $\pi^\pm\pi^0$ ). The correction is large only for the  $\rho$  and affects narrower resonances only very near resonance. The effect is part of the experimental data and as  $\omega$  and  $\phi$  have no charged partners there is nothing to be corrected in these cases. To include further mixing effects, like  $\omega - \rho^0$  mixing, one has to extend the Lagrangian and including all possible fields and their possible interactions, which leads to the HLS Lagrangian or a related effective model. For details I refer

to [9]. Nevertheless, let me add a few comments on the HLS approach:

Can global fits like our HLS implementation discriminate between incompatible data sets? The problem of inconsistent data is not a problem of whatever model, rather it is a matter of systematics of the measurements. Note that modeling is indispensable for interrelating different data channels. In the HLS global fit  $\tau$  data play a central role as they are *simple*, i.e. pure I=1, no singlet contribution, no  $\gamma - \rho^0 - \omega - \phi$  mixing. In fact,  $\tau$ -spectra supplemented with PDG isospin breaking, provide a good initial fit for most  $e^+e^-$ -data fits, which then are improved and optimized by iteration for a best simultaneous solution.

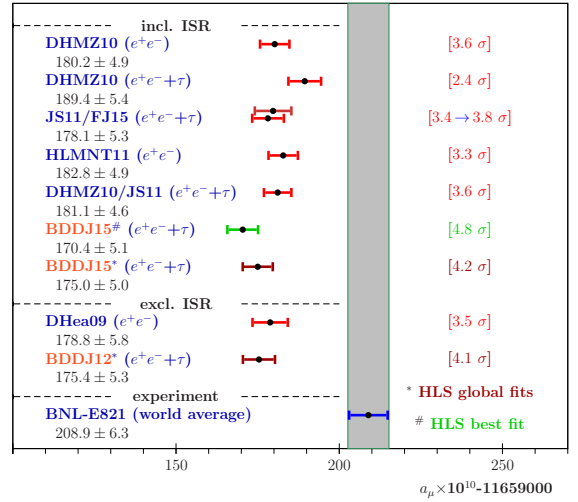


**Figure 12.** Comparison of recent LO  $a_\mu^{\text{had}}$  evaluations. Note that some results do not include  $\tau$  data. The HLS best fit BDDJ15# (NSK+KLOE10+KLOE12) does not include BaBar  $\pi\pi$  data [7], while BDDJ15\* does. JS11/FJ15 [35] is updated to include the new BES III data. Further points are BDDJ12 [5], DHMZ10 [59, 60], HLMNT11 [61] and DHea09 [39], (see also [51]).

Why do we get slightly lower results for HVP and with reduced uncertainties? BaBar data according to [59] are in good accord with Belle  $\tau$ -data, *before* correcting  $\tau$ -data for the substantial and quite unambiguous  $\gamma - \rho^0$  mixing effects! i.e. for the BaBar data alone there seems to be no  $\tau$  vs.  $e^+e^-$  puzzle, while the puzzle exists for all other  $e^+e^-$  data sets. This is a problem for the BaBar data. They are disfavored by our global fit! BaBar data rise the HVP estimate quite substantially towards the uncorrected  $\tau$  data value. In contrast the NSK, KLOE10/12 and the new BES-III data are in very good agreement with the  $\tau$  + PDG prediction [7], so they dominate the fit and give somewhat lower HVP result<sup>2</sup>! Since, besides the  $e^+e^-$  data, additional data constrain the HLS Lagrangian and its parameters, we find a reduced uncertainty and hence an increased significance.

What are the model (using specifically HLS) errors of our estimates? This is hard to say. Best do a corresponding analysis based on different implementations of the res-

<sup>2</sup>We are talking about a 1% shift, which is of the order of the size of the uncertainty.

onance Lagrangian approach. Try to include higher order corrections. However, the fit quality is surprisingly good and we do not expect that one has much flexibility. However, one can improve on photon radiation within a suitably extended HLS approach. Such processes have been implemented recently in the CARLOMAT Monte Carlo [62].

To conclude: our analysis is a first step in a direction which should allow for systematic improvements. A comparison of different estimates and leading uncertainties is shown in figure 12.

#### 4 HVP for the electron anomaly

An up-to-date reevaluation of hadronic VP effects to the electron  $g-2$  yields the results given in table 4. The present status is illustrated by the pie chart figure 13.

**Table 4.** 2015 update of HVP effects contributing to  $a_e$

$$\begin{aligned} a_e^{\text{had}(1)} &= (185.11 \pm 1.24) \times 10^{-14} \text{ (LO)} \\ a_e^{\text{had}(2)} &= (-22.15 \pm 0.16) \times 10^{-14} \text{ (NLO)} \\ a_e^{\text{had}(3)} &= (-2.80 \pm 0.02) \times 10^{-14} \text{ (NNLO) [54]} \end{aligned}$$

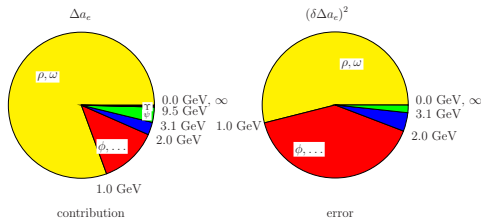


**Figure 13.** Electron  $g-2$ : contributions and square errors from different energy ranges.

On the theory side, the by far dominant QED contribution has been calculated to 5-loops [63] with the result

$$\begin{aligned} a_e^{\text{QED}} &= \frac{\alpha}{2\pi} - 0.328\,478\,444\,002\,55(33) \left(\frac{\alpha}{\pi}\right)^2 \\ &+ 1.181\,234\,016\,816(11) \left(\frac{\alpha}{\pi}\right)^3 \\ &- 1.9097(20) \left(\frac{\alpha}{\pi}\right)^4 + 9.16(58) \left(\frac{\alpha}{\pi}\right)^5. \end{aligned}$$

Together with the hadronic and weak contribution we get the SM prediction (incl.  $a_e^{\text{had,LbL}} = (3.7 \pm 0.5) \times 10^{-14}$ )

$$a_e^{\text{SM}} = a_e^{\text{QED}} + 1.725(12) \times 10^{-12} \text{ (hadr \& weak),}$$

which can be used for extracting  $\alpha_{\text{QED}}$  from  $a_e$  at unprecedented precision. Matching the theory prediction with the very precise experimental result of Gabrielse et al. [64]

$$a_e^{\text{exp}} = 0.001\,159\,652\,180\,73(28),$$

one extracts

$$\alpha^{-1}(a_e) = 137.0359991685(342)(68)(46)(24)[353],$$

which is close [85  $\rightarrow$  57] to the value

$$\alpha^{-1}(a_e) = 137.0359991657(342)[0.25 \text{ ppb}], \quad (9)$$

obtained by [63]. Note that the weak part has been reevaluated as

$$a_e^{\text{weak}} = 0.030 \times 10^{-12}, \quad (10)$$

which is replacing the value  $0.039 \times 10^{-12}$  which has been estimated in [65]. An inconsistency there has been noted by M. Passera [66].

The best test for new physics can be obtained by using  $\alpha$  from atomic interferometry [67]. With  $\alpha^{-1}(\text{Rb11}) = 137.035999037(91)[0.66 \text{ ppb}]$  as an input one finds

$$a_e^{\text{the}} = 0.001\,159\,652\,181\,87(77),$$

such that

$$a_e^{\text{exp}} - a_e^{\text{the}} = -1.14(0.82) \times 10^{-12}, \quad (11)$$

in good agreement. We know that the sensitivity to new physics is reduced by  $(m_\mu/m_e)^2 \cdot \delta a_e^{\text{exp}}/\delta a_\mu^{\text{exp}} \simeq 19$  relative to  $a_\mu$ . Nevertheless, one has to keep in mind that  $a_e$  is suffering less from hadronic uncertainties and thus may provide a safer test. Presently, the  $a_e$  prediction is limited by the, by a factor  $\delta\alpha(\text{Rb11})/\delta\alpha(a_e) \simeq 5.3$  less precise,  $\alpha$  available. Combining all uncertainties  $a_\mu$  is about a factor 43 more sensitive to new physics at present.

#### 5 HVP subtraction of $R_\gamma(s)$ : a problem of the DR method?

The full photon propagator is usually obtained by Dyson resummation of the  $1\text{pi}$  part (blob) as illustrated by figure 14. As we know this is a geometric series  $1 + x + x^2 +$

$$\begin{aligned} \text{Diagram: } \gamma \text{ (wavy line) with a blob } \circ \text{ (circle) } &= \text{Diagram: } \gamma \text{ (wavy line) with } \circ \text{ (circle) } + \text{Diagram: } \gamma \text{ (wavy line) with } \circ \text{ (circle) and } \circ \text{ (circle) } + \dots \\ i D'_\gamma(q^2) &\equiv \frac{-i}{q^2} + \frac{-i}{q^2} (-i\Pi_\gamma) \frac{-i}{q^2} + \frac{-i}{q^2} (-i\Pi_\gamma) \frac{-i}{q^2} (-i\Pi_\gamma) \frac{-i}{q^2} + \dots \\ &= \frac{-i}{q^2} \left\{ 1 + \left( \frac{-i\Pi_\gamma}{q^2} \right) + \left( \frac{-i\Pi_\gamma}{q^2} \right)^2 + \dots \right\} \\ &= \frac{-i}{q^2} \left\{ \frac{1}{1 + \frac{i\Pi_\gamma}{q^2}} \right\} = \frac{-i}{q^2 + i\Pi_\gamma(q^2)} = \frac{-i}{q^2} \frac{1}{1 + i\Pi'_\gamma(q^2)}. \end{aligned}$$

**Figure 14.** The Dyson summation of the photon self-energy.

$\dots = 1/(1-x)$  which only converges iff  $|x| < 1$ . Including the external e.m. couplings we have

$$i e^2 D'_\gamma(q^2) = \frac{-i}{q^2} \frac{e^2}{1 + i\Pi'_\gamma(q^2)}. \quad (12)$$

The effective charge thus is given by the well-known expression

$$\frac{e^2}{1 + i\Pi'_\gamma(s)} = \frac{e^2}{1 - \Delta\alpha(s)} = e^2(s). \quad (13)$$

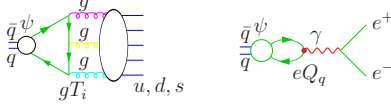


**Figure 15.** OZI suppressed strong decays let e.m. interaction look to be almost of equal strength.

Usually,  $\Delta\alpha(s)$  is a correction i.e  $\Delta\alpha(s) \ll 1$  and the Dyson series converges well. Indeed for any type of perturbative effects no problem is encountered (besides possible Landau poles). For non-perturbative strong interaction physics there are exceptions. One would expect that, if there are problems, one would encounter them at low energy, but for the  $\rho$ , the  $\omega$  and the  $\phi$ , in spite of huge resonance enhancements, the hadronic VP contributions to the running charge are small relative to unity, as the effect is suppressed by the e.m. coupling  $e^2$ . The exception, surprisingly, we find at pretty high energies, at the narrow OZI suppressed resonances, which are extremely sharp, because they lie below corresponding  $q\bar{q}$ -thresholds. While the strong interaction appears heavily suppressed (3 gluons exchange) the electromagnetic channel (1 photon exchange) appears almost as strong as the strong one (see figure 15). Actually,  $\Gamma_{ee}$  is not much smaller than  $\Gamma_{\text{QCD}}$  (i.e strong decays). This phenomenon shows up for the resonances  $J/\psi$ ,  $\psi_2$ ,  $\Upsilon_1$ ,  $\Upsilon_2$  and  $\Upsilon_3$ . The imaginary parts from the narrow resonances read

$$\text{Im}\Pi'_\gamma(s) = \frac{\alpha}{3} R_\gamma(s) = \frac{3}{\alpha} \frac{\Gamma_{ee}}{\Gamma} \quad (14)$$

at peak, causing the sharp spikes, which are seen only by appropriate high resolution scans, as we know. Let  $\alpha(s)$  denotes the real  $\alpha(s) = \alpha/(1 + \text{Re}\Pi'_\gamma(s))$ , we note that,

$$|1 + \Pi'_\gamma(s)|^2 - (\alpha/\alpha(s))^2 = (\text{Im}\Pi'_\gamma(s))^2$$

and at  $\sqrt{s} = M_R$  values for the the different resonances are given by  $1.23 \times 10^{-3}$  ( $\rho$ ),  $2.76 \times 10^{-3}$  ( $\omega$ ),  $1.56 \times 10^{-2}$  ( $\phi$ ), 594.81 ( $J/\psi$ ), 9.58 ( $\psi_2$ ),  $2.66 \times 10^{-4}$  ( $\psi_3$ ), 104.26 ( $\Upsilon_1$ ), 30.51 ( $\Upsilon_2$ ) and 55.58 ( $\Upsilon_3$ ). This shows that near QZI suppressed resonances the Dyson series cannot converge. So we have a problem with the dispersive approach, which requires  $R_\gamma(s) \propto \text{Im}\Pi'_\gamma(s)$  as an input. What is measured by an experiment is the full propagator, the summed up Dyson series,  $Z = |1/(1-x)|^2$ , but we cannot extract  $x$  from that since for  $|x| \geq 1$  the observable  $Z$  has no representation in terms of  $x$ . Remember that the object required in the DR is the undressed  $R_\gamma(s)$  in (1), which cannot be measured itself, rather we have to extract ( $x = -\Pi'_\gamma(s)$ )

$$R_\gamma^{\text{bare}} = R_\gamma^{\text{phys}} |1 + \Pi'_\gamma(s)|^2. \quad (15)$$

Locally, near OZI suppressed resonances, the usual iterative procedure of getting  $R_\gamma^{\text{bare}}$  does not converge! The way out usually practiced is to utilize the smooth space-like charge, i.e.  $\bar{R}_\gamma^{\text{bare}} = R_\gamma^{\text{phys}} |1 + \Pi'_\gamma(-s)|^2$ , expected to do the undressing “in average”. This actually does not look too wrong as we see in figure 16. Nevertheless, I see a problem her, not only for the interpretation of resonance data, where one would wish to be able to disentangle electromagnetic form strong interaction effects.

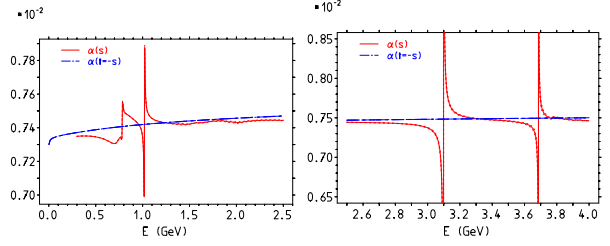


**Figure 16.** Time-like vs. space-like effective finestructure constant  $\alpha$  as a function of the energy  $E$ :  $\alpha(s)$  in the mean follows  $\alpha(t = -s)$  ( $s = E^2$ ). Note that the smooth space-like effective charge agrees rather well with the non-resonant “background” above the  $\phi$  (kind of duality).

For what concerns the proper extraction of the hadronic effects contributing to the running of  $\alpha_{\text{QED}}$  and to  $a_\mu^{\text{had}}$ , I see no proof that this cannot produce non-negligible shifts!

Fortunately, experimental progress is in sight here: KLOE 2015 [68] has a first direct measurements of the time-like complex running  $\alpha_{\text{QED}}(s)$ ! Similar measurements for the  $J/\psi$  and other ultra-narrow resonances should be possible with BES III. It is a fundamental problem! An interesting possibility in this respect is a novel approach to determine  $a_\mu^{\text{had}}$  form a direct space-like measurement of  $\alpha(-Q^2)$  as proposed in [69, 70], recently.

## 6 A comment on axial exchanges in HLbL

The Landau-Yang theorem says that the amplitude  $\mathcal{A}(\text{axial meson } \gamma\gamma)|_{\text{on-shell}} = 0$ , e.g.  $Z^0 \rightarrow \gamma\gamma$  is forbidden, while  $Z^0 \rightarrow \gamma e^+ e^-$  is allowed as one of the photons is off-shell. For HLbL such type of contribution has been estimated in [17] to be rather large, which raised the question: Why  $a_\mu[a_1, f'_1, f_1] \sim 22 \times 10^{-11}$  is so large? From the data side we know, untagged  $\gamma\gamma \rightarrow f_1$  shows no signal, while single-tag  $\gamma^* \gamma \rightarrow f_1$  is strongly peaked when  $Q^2 \gg m_{f_1}^2$ . The point: the contribution from axial mesons has been calculated assuming a symmetric form-factors under exchange of the two photon momenta. This violates the Landau-Yang theorem, which requires an antisymmetric form-factor. In fact antisymmetrizing the form-factor adopted in [17] reduces the contribution by a factor about 3, and the result agrees with previous findings [1, 2] and with the more recent result [20]. As a result one finds that the estimate  $a_\mu^{\text{HLbL,LO}} = (116 \pm 39) \times 10^{-11}$  accepted in [65] must be replaced by

$$a_\mu^{\text{HLbL,LO}} = (102 \pm 39) \times 10^{-11}. \quad (16)$$

This also requires a modification of the result advocated in [71]. The evaluation of the axialvector mesons contribution, taking a Landau-Yang modified (i.e, antisymmetrized) Melnikov-Vainshtein form-factors yields [72]

$$a_\mu[a_1, f'_1, f_1] \sim (7.51) = [1.89 + 5.04 + 0.58] \pm 2.71 \times 10^{-11}, \quad (17)$$

where ideal mixing and nonet symmetry results have been averaged. In fact, the sum of the contributions from the  $f_1$  and  $f'_1$  depends little on the mixing scheme. The result supersedes  $a_\mu[a_1, f'_1, f_1] \sim 22(5) \times 10^{-11}$  we included in [65].

## 7 Theory vs. experiment: do we see New Physics?

**Table 5.** A list of small shifts in theory [in units  $10^{-11}$ ]. The error from new entries in the list reduces from the old 5 to 3.6.

New contribution	$a_\mu$	Reference
Old axial exchange HLbL	$22 \pm 5$	[17]
New axial exchange HLbL	$7.51 \pm 2.71$	[20, 72]
NNLO HVP	$12.4 \pm 0.1$	[54]
NLO HLbL	$3 \pm 2$	[73]
Tensor exchange HLbL	$1.1 \pm 0.1$	[20]
Total change	$+2.0 \pm 3.4$	

Here I briefly summarize what is new and where we are. Some new results/evaluations are collected in table 5. We finally compare the SM prediction for  $a_\mu$  with its experimental value [77] in table 6, which also summarizes the present status of the different contributions to  $a_\mu$ . A deviation between 3 and 5  $\sigma$  is persisting and was slightly increasing. Resonance Lagrangian models, like the HLS model, provide clear evidence that there is no  $\tau$  version HVP which differs from the  $e^+e^-$  data result. This consolidates a larger deviation  $\Delta a_\mu = a_\mu^{\text{exp}} - a_\mu^{\text{the}}$ . Also the decrease of the axial HLbL contribution goes in this direction, it is compensated however by the new NNLO HVP result. What represents the 4  $\sigma$  deviation: new physics? Is it a statistical fluctuation? Are we underestimating uncertainties (experimental, theoretical)? Do experiments measure what theoreticians calculate? I refer to [78] for possible interpretations and conclusions.

## 8 Outlook

Although progress is slow, there is evident progress in reducing the hadronic uncertainties, most directly by progress in measuring the relevant hadronic cross-sections. Near future progress we expect from BINP Novosibirsk/Russia and from IHEP Beijing/China. Energy scan as well as ISR measurement of cross-sections in the region from 1.4 to 2.5 GeV are most important to reduce the errors to a level competitive with the factor 4 improvement achievable by the upcoming new muon  $g-2$  experiments at Fermilab/USA and at JPAC/Japan [56]. Also BaBar data are still being analyzed and are important for improving the results. Promising is that lattice QCD evaluations come closer to be competitive [15].

## Acknowledgements

I thank Z. Zhang for helpful discussions on the isospin breaking corrections and M. Benayoun for close collaboration on HLS driven estimates of  $a_\mu^{\text{had}}$ .

## References

[1] M. Hayakawa, T. Kinoshita, A. I. Sanda, Phys. Rev. Lett. **75**, 790 (1995); Phys. Rev. D **54**, 3137 (1996)

**Table 6.** Standard model theory and experiment comparison [in units  $10^{-10}$ ].

Contribution	Value	Error	Reference
QED at 5-loops	11 658 471 . 8851	0 . 036	[55, 74, 75]
LO HVP	688 . 91	3 . 52	(3)
NLO HVP	-9 . 917	0 . 100	table 2
NNLO HVP	1 . 225	0 . 012	[54], table 3
HLbL	10 . 6	3 . 9	[65, 72], table 5
EW at 2-loops	15 . 40	0 . 10	[25, 26, 76]
Theory	11 659 178 . 10	5 . 26	–
Experiment	11 659 209 . 1	6 . 3	[77] (updated)
Exp-The 3.8 $\sigma$	31 . 0	8 . 2	–

[2] J. Bijnens, E. Pallante, J. Prades, Phys. Rev. Lett. **75**, 1447 (1995) [Erratum-ibid. **75**, 3781 (1995)]; Nucl. Phys. B **474**, 379 (1996); [Erratum-ibid. **626**, 410 (2002)];  
J. Bijnens, J. Prades, Mod. Phys. Lett. A **22**, 767 (2007)

[3] J. Bijnens, these proceedings

[4] S. Eidelman, F. Jegerlehner, Z. Phys. C **67**, 585 (1995); F. Jegerlehner, Nucl. Phys. (Proc. Suppl.) C **51**, 131 (1996); J. Phys. G **29**, 101 (2003); Nucl. Phys. Proc. Suppl. **126**, 325 (2004)

[5] M. Benayoun, P. David, L. DelBuono, F. Jegerlehner, Eur. Phys. J. C **72**, 1848 (2012)

[6] M. Benayoun, P. David, L. DelBuono, F. Jegerlehner, Eur. Phys. J. C **73**, 2453 (2013)

[7] M. Benayoun, P. David, L. DelBuono, F. Jegerlehner, arXiv:1507.02943 [hep-ph]

[8] F. Jegerlehner, Acta Phys. Polon. B **44**, Vol.11, 2257 (2013)

[9] M. Benayoun, these proceedings.

[10] P. Boyle, L. Del Debbio, E. Kerrane, J. Zanotti, Phys. Rev. D **85** (2012) 074504

[11] X. Feng et al., Phys. Rev. D **88**, 034505 (2013)

[12] C. Aubin, T. Blum, M. Golterman, S. Peris, Phys. Rev. D **88**, 074505 (2013)

[13] A. Francis et al., arXiv:1411.3031 [hep-lat]

[14] R. Malak et al. [Budapest-Marseille-Wuppertal Col- lab.], PoS LATTICE **2014**, 161 (2015)

[15] M. Petschlies, these proceedings.

[16] M. Knecht, A. Nyffeler, Phys. Rev. D **65**, 073034 (2002)

[17] K. Melnikov, A. Vainshtein, Phys. Rev. D **70**, 113006 (2004)

[18] M. Knecht, Nucl. Part. Phys. Proc. **258-259**, 235 (2015); and these proceedings

[19] A. Nyffeler, these proceedings

[20] V. Pauk, M. Vanderhaeghen, Eur. Phys. J. C **74**, 3008 (2014)

[21] G. Colangelo et al., Phys. Lett. B **738**, 6 (2014)

[22] M. Procura, these proceedings

[23] T. Blum, S. Chowdhury, M. Hayakawa, T. Izubuchi, Phys. Rev. Lett. **114**, 012001 (2015)

[24] Ch. Lehner, these proceedings

[25] M. Knecht, S. Peris, M. Perrottet, E. de Rafael, JHEP **0211**, 003 (2002)



- [26] A. Czarnecki, W. J. Marciano, A. Vainshtein, Phys. Rev. D **67**, 073006 (2003) [Erratum-ibid. D **73**, 119901 (2006)]
- [27] R. R. Akhmetshin et al. [CMD-2 Collab.], Phys. Lett. B **578**, 285 (2004)
- [28] V. M. Aulchenko et al. [CMD-2 Collab.], JETP Lett. **82**, 743 (2005) [Pisma Zh. Eksp. Teor. Fiz. **82**, 841 (2005)]; R. R. Akhmetshin et al., JETP Lett. **84**, 413 (2006) [Pisma Zh. Eksp. Teor. Fiz. **84**, 491 (2006)]; Phys. Lett. B **648**, 28 (2007)
- [29] M. N. Achasov et al. [SND Collab.], J. Exp. Theor. Phys. **103**, 380 (2006) [Zh. Eksp. Teor. Fiz. **130**, 437 (2006)]
- [30] A. Aloisio et al. [KLOE Collab.], Phys. Lett. B **606**, 12 (2005);  
F. Ambrosino et al. [KLOE Collab.], Phys. Lett. B **670**, 285 (2009)
- [31] F. Ambrosino et al. [KLOE Collab.], Phys. Lett. B **700**, 102 (2011)
- [32] D. Babusci et al. [KLOE Collab.], Phys.Lett. **B720**, 336 (2013)
- [33] B. Aubert et al. [BABAR Collab.], Phys. Rev. Lett. **103**, 231801 (2009); J. P. Lees et al., Phys.Rev. **D86**, 032013 (2012)
- [34] M. Ablikim et al. [BESIII Collab.], arXiv:1507.08188 [hep-ex]
- [35] F. Jegerlehner, R. Szafron, Eur. Phys. J. C **71**, 1632 (2011)
- [36] R. Alemany, M. Davier, A. Höcker, Eur. Phys. J. C **2**, 123 (1998)
- [37] M. Davier, S. Eidelman, A. Höcker, Z. Zhang, Eur. Phys. J. C **27**, 497 (2003); Eur. Phys. J. C **31**, 503 (2003)
- [38] S. Ghozzi, F. Jegerlehner, Phys. Lett. B **583**, 222 (2004)
- [39] M. Davier et al., Eur. Phys. J. C **66**, 127 (2010)
- [40] Z. Zhang, these proceedings.
- [41] R. Barate et al. [ALEPH Collab.], Z. Phys. C **76**, 15 (1997); Eur. Phys. J. C **4**, 409 (1998); S. Schael et al. [ALEPH Collab.], Phys. Rept. **421**, 191 (2005)
- [42] M. Davier et al., Eur.Phys.J. **C74**, 2803 (2014)
- [43] K. Ackerstaff et al. [OPAL Collab.], Eur. Phys. J. C **7**, 571 (1999)
- [44] S. Anderson et al. [CLEO Collab.], Phys. Rev. D **61**, 112002 (2000)
- [45] M. Fujikawa et al. [Belle Collab.], Phys. Rev. D **78**, 072006 (2008)
- [46] R. Akhmetshin et al. [CMD-3 Collab.], Phys.Lett. **B723**, 82 (2013)
- [47] M. Achasov et al. [SND Collab.], Phys.Rev. **D88**, 054013 (2013)
- [48] J. Lees et al. [BABAR Collab.], Phys.Rev. **D87**, 092005 (2013)
- [49] J. Lees et al. [BABAR Collab.], Phys.Rev. **D88**, 032013 (2013)
- [50] J. Lees et al. [BABAR Collab.], Phys.Rev. **D89**, 092002 (2014)
- [51] M. Davier, Nucl. Part. Phys. Proc. **260**, 102 (2015)
- [52] J. Z. Bai et al. [BES Collab.], Phys. Rev. Lett. **84**, 594 (2000); Phys. Rev. Lett. **88**, 101802 (2002);  
M. Ablikim et al., Phys. Lett. B **677**, 239 (2009)
- [53] B. Krause, Phys. Lett. B **390** (1997) 392
- [54] A. Kurz, T. Liu, P. Marquard, M. Steinhauser, Phys.Lett. **B734**, 144 (2014)
- [55] M. Steinhauser, these proceedings
- [56] D. Hertzog, these proceedings.
- [57] M. Bando, T. Kugo, K. Yamawaki, Phys. Rept. **164**, 217 (1988);  
M. Harada, K. Yamawaki, Phys. Rept. **381**, 1 (2003)
- [58] M. Benayoun et al., Eur. Phys. J. **C55**, 199 (2008);  
M. Benayoun, P. David, L. DelBuono, O. Leitner, Eur. Phys. J. **C65**, 211 (2010); Eur. Phys. J. **C68**, 355 (2010)
- [59] M. Davier et al., Eur. Phys. J. **C66**, 1 (2009)
- [60] M. Davier et al., Eur. Phys. J. **C71**, 1515 (2011)
- [61] K. Hagiwara et al., J. Phys. **G38**, 085003 (2011)
- [62] K. Kołodziej, Comput. Phys. Commun. **196**, 563 (2015)
- [63] T. Aoyama, M. Hayakawa, T. Kinoshita, M. Nio, Phys. Rev. Lett. **109**, 111807 (2012)
- [64] G. Gabrielse et al., Phys. Rev. Lett. **97** (2006) 030802 [Erratum-ibid. **99** (2007) 039902]
- [65] F. Jegerlehner, A. Nyffeler, Phys. Rept. **477**, 1 (2009)
- [66] M. Passera private communication
- [67] R. Bouchendira et al., Phys. Rev. Lett. **106** (2011) 080801
- [68] The KLOE Collaboration, to be published
- [69] C. M. Carloni et al., Phys. Lett. B **746**, 325 (2015)
- [70] L. Trentadue, these proceedings
- [71] J. Prades, E. de Rafael, A. Vainshtein, Adv. Ser. Direct. High Energy Phys. **20**, 303 (2009)
- [72] F. Jegerlehner, Talk at the MITP Workshop “Hadronic contributions to the muon anomalous magnetic moment”, 1-5 April 2014, Waldthausen Castle near Mainz, and to be published
- [73] G. Colangelo et al., Phys.Lett. **B735**, 90 (2014)
- [74] T. Aoyama, M. Hayakawa, T. Kinoshita, M. Nio, Phys. Rev. Lett. **109**, 111808 (2012)
- [75] A. Kurz et al., Phys. Rev. D **92**, 073019 (2015)
- [76] C. Gnendiger, D. Stöckinger, H. Stöckinger-Kim, Phys. Rev. D **88**, 053005 (2013)
- [77] G. W. Bennett et al. [Muon g-2 Collab.], Phys. Rev. D **73** (2006) 072003
- [78] D. Stöckinger, these proceedings